This article was downloaded by: [Chongqing University]
On: 14 February 2014, At: 14:56
Publisher: Taylor & Francis
Informa Ltd Registered in England and Wales Registered Number: 1072954 Registered office: Mortimer House, 37-41 Mortimer Street, London W1T 3JH, UK

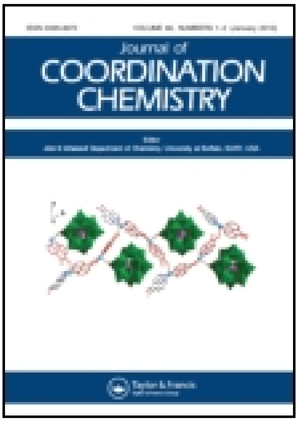

Journal of Coordination Chemistry
Publication details, including instructions for authors and subscription information:
http://www.tandfonline.com/loi/gcoo20

Copper(II) complexes of a new tetradentate bis-benzimidazolyl diamide ligand with disulfanediyl linker: synthesis, characterization, and oxidation of some pyridyl, napthyl, and benzyl alcohols

Nidhi Tyagi[a], Ravinder Kumar[a], Kuldeep Mahiya[a] & Pavan Mathur[a]
[a] Department of Chemistry, University of Delhi, Delhi, India

Accepted author version posted online: 16 Aug 2013.Published online: 22 Oct 2013.

To cite this article: Nidhi Tyagi, Ravinder Kumar, Kuldeep Mahiya & Pavan Mathur (2013) Copper(II) complexes of a new tetradentate bis-benzimidazolyl diamide ligand with disulfanediyl linker: synthesis, characterization, and oxidation of some pyridyl, napthyl, and benzyl alcohols, Journal of Coordination Chemistry, 66:19, 3335-3348, DOI: 10.1080/00958972.2013.835403

To link to this article: http://dx.doi.org/10.1080/00958972.2013.835403

PLEASE SCROLL DOWN FOR ARTICLE

Taylor & Francis makes every effort to ensure the accuracy of all the information (the "Content") contained in the publications on our platform. However, Taylor & Francis, our agents, and our licensors make no representations or warranties whatsoever as to the accuracy, completeness, or suitability for any purpose of the Content. Any opinions and views expressed in this publication are the opinions and views of the authors, and are not the views of or endorsed by Taylor & Francis. The accuracy of the Content should not be relied upon and should be independently verified with primary sources of information. Taylor and Francis shall not be liable for any losses, actions, claims, proceedings, demands, costs, expenses, damages, and other liabilities whatsoever or howsoever caused arising directly or indirectly in connection with, in relation to or arising out of the use of the Content.

This article may be used for research, teaching, and private study purposes. Any substantial or systematic reproduction, redistribution, reselling, loan, sub-licensing, systematic supply, or distribution in any form to anyone is expressly forbidden. Terms &

Journal of Coordination Chemistry, 2013
Vol. 66, No. 19, 3335–3348, http://dx.doi.org/10.1080/00958972.2013.835403

Copper(II) complexes of a new tetradentate *bis*-benzimidazolyl diamide ligand with disulfanediyl linker: synthesis, characterization, and oxidation of some pyridyl, napthyl, and benzyl alcohols

NIDHI TYAGI, RAVINDER KUMAR, KULDEEP MAHIYA and PAVAN MATHUR*

Department of Chemistry, University of Delhi, Delhi, India

(*Received 6 June 2013; accepted 31 July 2013*)

The *bis*-benzimidazolyl diamide ligand 3,3′-disulfanediyl-*bis*-(*N*-((1*H*-benzo[d]imidazol-2-yl)methyl) propanamide) (L) having N, S, and O donors has been synthesized and utilized to prepare copper(II) complexes of general composition [Cu(L)X]·X·nH$_2$O, where X is Cl$^-$ or NO$_3^-$. Ligands and complexes were characterized by elemental analysis, UV–visible, IR spectroscopy, ^{1}H NMR, mass spectrometry, conductance, electron paramagnetic resonance, cyclic voltammetry, fluorescence, single-crystal, and PXRD. [Cu(L)(NO$_3$)]NO$_3$·H$_2$O crystallizes in the monoclinic *C2/c* space group with one molecule in the asymmetric unit. Copper adopts a distorted octahedral geometry with four coordination sites occupied by the ligand and two sites by a bidentate nitrate. [Cu(L)(NO$_3$)] NO$_3$·H$_2$O has been utilized as a catalyst to oxidize alcohols with *tert*-butyl hydroperoxide as an alternative source of oxygen. The oxidized products have been characterized by GCMS.

Keywords: Copper(II) complexes; N, S, and O donor benzimidazolyl diamide ligands; Crystal structure; Galactose oxidase

1. Introduction

Transition metal complex-catalyzed oxidation of organic compounds has been extensively investigated. Introduction of efficient catalysts for the selective insertion of one oxygen from oxygen donors (like O$_2$, H$_2$O$_2$, t-BuOOH, or NaOCl) into various organic molecules, under mild conditions, has been a challenge in chemical catalysis [1]. The search for efficient oxidation catalysts is increasingly being guided by considering the active site structures of metalloenzymes. An example is the fungal enzyme galactose oxidase (GOase) catalyzing selectively aerobic oxidation of a wide range of primary alcohols to the corresponding aldehydes [2]. Stack and co-workers described the use of a functional mononuclear Cu(II) model compound as a catalyst of aerobic oxidation of activated benzyl and allylic alcohols with high turnover numbers in the presence of an excess of the base (alkoxide) as co-catalyst [3], while Wieghardt and co-workers reported a mononuclear 2,2′-thio-*bis*-(phenolato) triethylamine copper(II) compound that oxidized both primary and secondary alcohols to the corresponding aldehydes and ketones, respectively, and/or to 1,2-glycol derivatives [4, 5]. Oxidation of benzyl alcohol has been widely discussed by

---

*Corresponding author. Email: pavanmat@yahoo.co.in

Valodkar *et al.* using polymer-Cu(II) metal complexes as catalysts and *tert*-butyl hydroperoxide (TBHP) as oxidant [6].

Both homogenous and heterogeneous catalysts based on various metals including Mn, V, Fe, Ni, Cu, Ag, and Au are effective in the oxidation of many alcohols [7]. Ag and Au [8, 9] catalysts are reported in heterogeneous media while copper is reported to be efficient under both homogeneous and heterogeneous conditions [10a,b].

In the present research, a $N_2O_2S_2$ donor benzimidazolyl-based ligand and its copper(II) complexes have been synthesized and characterized. One Cu(II) complex has been used as the homogeneous catalyst in the oxidation of alcohols to carbonyl compounds and carboxylic acids using t-butyl hydroperoxide as a source of oxygen.

2. Experimental

2.1. *Materials*

All solvents used were of HPLC grade. 3,3′-Thiodipropionic acid, 3-pyridyl carbinol, 1,2,3,4-tetrahydronaphthol, 4-methoxybenzyl alcohol, Geraniol, and 4-nitrobenzyl alcohol were obtained from Sigma–Aldrich. All other chemicals were obtained from commercial sources and used as received. 2-Aminomethyl benzimidazolyl dihydrochloride was prepared following the procedure reported by Cescon and Day [11]. As required, all safety precautions, were adhered to while handling the above chemicals.

2.2. *Physical measurements*

Carbon, hydrogen, nitrogen, and sulfur were estimated using an elemental analyzer at USIC, University of Delhi, Delhi. Electronic spectra were recorded in HPLC-grade DMF on a Shimadzu 1601 spectrophotometer from 200 to 1100 nm. IR spectra were recorded in the solid state as KBr pellets on a Perkin–Elmer FTIR-2000 spectrometer. ^{1}H NMR (400 MHz) spectra of ligands were recorded in DMSO-d_6 on a JEOL ECX-400P NMR spectrometer at the Department of Chemistry, University of Delhi, Delhi. Conductance values were measured on a digital conductivity bridge from Popular Traders, India (Model: PT-825) at the Department of Chemistry, University of Delhi. Electrochemistry was studied on a BAS CV 50 W electrochemical analysis system at the Department of Chemistry, University of Delhi, Delhi. Tetrabutyl ammonium perchlorate (0.1 M) was used as the supporting electrolyte. A three-electrode configuration composed of Pt-disk working electrode (3.1 mm^2 area), a Pt-wire counter electrode, and a Ag/AgNO$_3$ reference electrode was used for the measurements. $E_{1/2}$ of ferrocene was + 56 mV. ESI-MS were obtained from CDRI, Lucknow, India. X-band EPR spectra were recorded on a Bruker Spectrospin with a variable temperature liquid nitrogen cryostat at 120 K at IIT Bombay, India. GCMS spectra were recorded at Advanced Instrumentation & Research Facility, Jawaharlal Nehru University, New Delhi, on a GCMS-QP 2010(plus) Shimadzu instrument. Fluorescence spectra were recorded in methanol on a Varian CARY Eclipse fluorescence spectrophotometer. Powder X-ray diffraction patterns were recorded using a high resolution D8 discover Bruker X-ray diffractometer equipped with a point detector (scintillation counter), employing monochromated Cu–Kα_1 radiation obtained through a globel mirror with a scan rate of 1.0 s/step and step size of 0.02° at 298 K from $2\theta = 10$–40. Single-crystal diffraction data were collected on an X-Calibur single-crystal X-ray diffractometer having a CCD camera at the University of Delhi, Delhi, India.

2.3. *Synthesis of 3,3′-disulfanediyl-bis (N-((1H-benzo [d] imidazol-2-yl) methyl) propanamide) (L)*

L was prepared following the procedure reported by Mathur *et al.* [12]. A solution of 2-aminomethyl benzimidazolyl dihydrochloride (5.0 g, 22.7 M) and 3,3′-dithiodipropionic acid (2.38 g, 11.4 M) in 20 mL pyridine was stirred for 5 min until a white precipitate was obtained (during the reaction pyridine forms pyridine hydrochloride). Then, triphenyl phosphate (6.38 mL, 22.7 M) was added to the reaction mixture at a temperature of 50 °C and the temperature was slowly raised to 80–85 °C. Within half an hour, the precipitate redissolved and the clear solution was stirred for 30 h. The resulting orange-brown solution was allowed to cool and washed with saturated $NaHCO_3$ solution in a separating funnel until no effervescence could be seen. Then, it was washed with water 2–3 times. While washing, the oil solidified into a light yellow solid (scheme 1). Upon further washing with acetone, the solid turned white. This was dried and recrystallized by hot methanol:H_2O (1:1). The recrystallized white product was filtered, washed with cold water, and dried in air. Yield: 55%, Melting point: 185–186 °C. Anal. found for $C_{22}H_{24}N_6O_2S_2 \cdot CH_3OH$: C, 54.5; H, 6.1; N, 17.4; S, 12.0%. Calcd: C, 55.2; H, 5.6; N, 16.8; S, 12.8%. UV/vis spectrum (DMF) λ_{max}, nm (log ε, M^{-1} cm^{-1}) = 283 (4.35), 276 (4.38). IR (KBr pellets, cm^{-1}):ν = 3310 (O–H), 3235 (N–H amide), 3062 (N–H benzimidazole), 1646 (C=O amide I), 1540 (C–N amide II), 1431 (C=N–C=C (benzimidazole)), 740 (C=C benzene), 677 (C–S). ^{1}H-NMR (DMSO-d_6, ppm) δ: 12.2 (s, 2H), 8.70–8.67 (t, 2H), 7.53–7.45 (d, 4H), 7.14–7.13 (q, 4H), 4.50–4.47 (d, 4H), 2.97–2.93 (t, 4H), 2.63–2.61 (t, 4H). ESI/MS$^+$ (m/e): 468.

2.4. *Synthesis of copper(II) complexes*

2.4.1. [Cu(L)Cl]Cl. To a solution of L (100 mg, 0.21 mM) in 10 mL CH_3OH, a methanolic solution (5 mL) of $CuCl_2 \cdot 2H_2O$ (36.4 mg, 0.21 mM) was added. The reaction mixture was stirred for 4 h at room temperature. The reaction mixture was then concentrated on a rotary evaporator and kept in a refrigerator for a few hours, when a green product separated. The product was filtered and washed with cold MeOH. Yield: 50%. Anal. found for

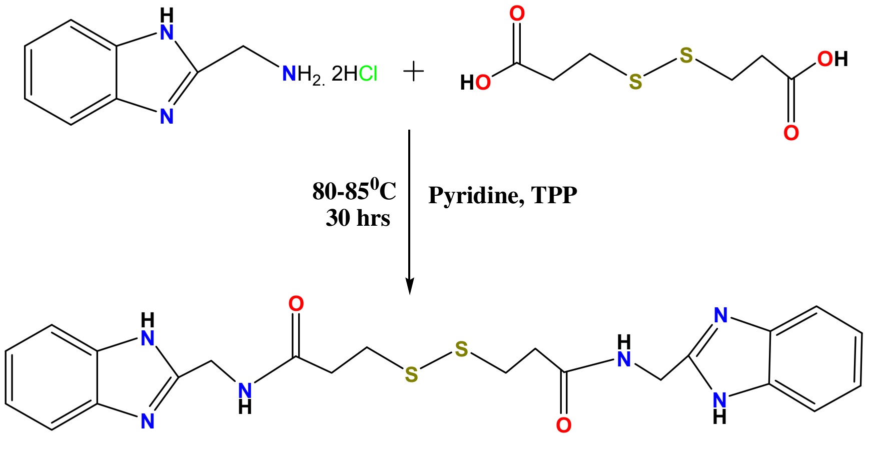

Scheme 1. Synthesis of 3,3′-disulfanediyl-*bis*(*N*-((1*H*-benzo[d]imidazol-2-yl)methyl)propanamide) (L).

$C_{22}H_{24}N_6O_2S_2Cl_2Cu{\cdot}2H_2O$ (638.5): C, 40.7; H, 4.2; N, 12.7; S, 10.0%. Calcd: C, 41.3; H, 4.3; N, 13.1; S, (10.0) %. UV/vis spectrum (DMF) λ_{max}, nm (log ε, M^{-1} cm^{-1}): 276 (4.10), 282 (4.06), 760 (1.88). IR (KBr pellets, cm^{-1}): ν = 3421 (O–H), 3250 (N–H amide), 3065 (N–H (benzimidazole)), 1654 (C=O amide I), 1540 (C–N amide II), 1455 (C=N–C=C (benzimidazole)), 745 (C=C benzene), ν = 663 (C–S).

2.4.2. $[Cu(L)NO_3]NO_3$. The procedure was similar to [Cu(L)Cl]Cl except that $Cu(NO_3)_2{\cdot}3H_2O$ (51.6 mg, 0.21 mM) was used instead of $CuCl_2{\cdot}2H_2O$ for complexation. The reaction mixture was then kept for crystallization. After a few days, green crystals were obtained. Yield: 65%. Anal. found for $C_{22}H_{24}N_8O_8S_2Cu{\cdot}H_2O$ (673.5): C, 38.8; H, 4.1; N, 16.5; S, 9.3%. Calcd: C, 39.1; H, 3.9; N, 16.6; S, 9.5%. UV/vis (DMF) λ_{max}, nm (log ε M^{-1} cm^{-1}): 275 (4.03), 282 (3.98), 720 (1.79). IR (KBr pellets, cm^{-1}): ν = 3450 (O–H), 3257 (N–H amide), 3058 (N–H (benzimidazole)), 1625 (C=O amide I), 1543 (C–N amide II), 1453 (C=N–C=C (benzimidazole)), 1384 (N–O), 745 (C=C benzene), 663 (C–S). IR (KBr pellets, cm^{-1}): ν = 3460 (O–H), 3290 (N–H amide), 1661 (C=O amide I), 1538 (C–N amide II), 1432 (C=N–C=C benzimidazole), 747 (C=C benzene), 670 (C–S).

2.5. *X-ray crystallography*

Single crystals of $[Cu(L)NO_3]NO_3{\cdot}H_2O$ suitable for X-ray diffraction studies were grown by slow evaporation in methanol at room temperature. The intensity data were collected at 298 K on an X-calibur CCD diffractometer with graphite monochromated Mo/Kα radiation.

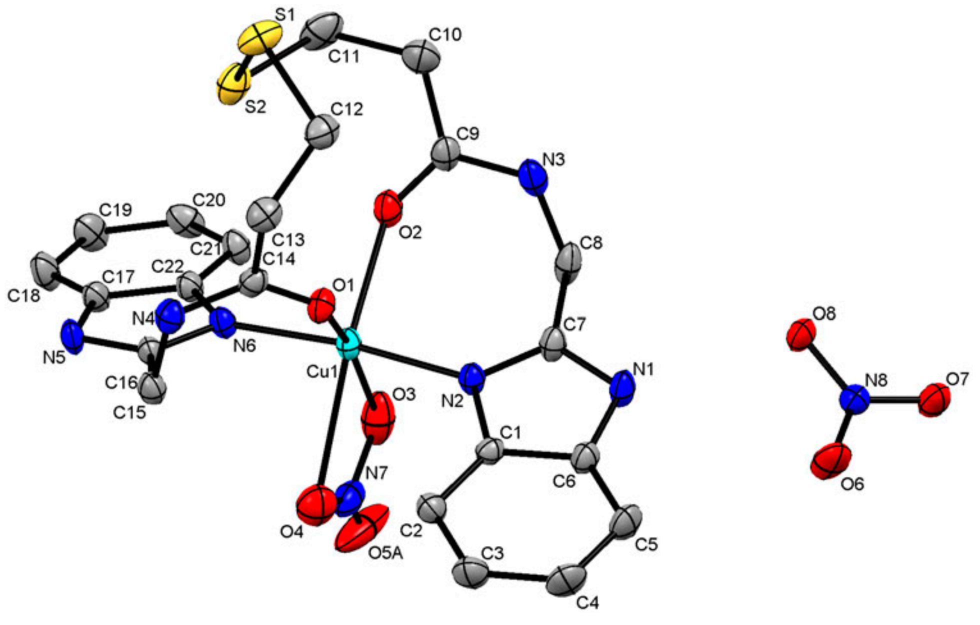

Figure 1. ORTEP diagram of $[Cu(L)(NO_3)]NO_3{\cdot}H_2O$ drawn in 20% thermal probability ellipsoids showing the atom numbering scheme. Hydrogen and lattice water have been removed for clarity. Only one site of disordered oxygen (O5A) of bound nitrate is shown.

A total of 40,794 reflections were measured of which 5543 were unique and 4113 were considered observed ($I > 2\sigma(I)$). The data were corrected for Lorentz and polarization effects and multi-scan absorption correction was applied. The structure was solved by direct methods using SHELXS-97 [13a] and refined by full-matrix least-squares refinement on F^2 using SHELXL-97 [13a]. All calculations were done with the help of WinGX package of crystallographic programs [13b]. All non-hydrogen atoms except the disordered lattice water were refined anisotropically. All hydrogens were fixed geometrically with U_{iso} values of 1.2 times the U_{iso} values of their respective carrier. Hydrogens on lattice water were not located. The final residual indices are R 0.0779, Rw 0.2236 for the observed and R 0.1055, Rw 0.2431 for all reflections using 378 parameters and 2 restraints. Thermal ellipsoid plot (ORTEP) for $[Cu(L)NO_3]NO_3$ is shown in figure 1. Crystal and structure refinement data and selected geometrical parameters are summarized in tables 1 and 2, respectively.

Table 1. Crystal data and structure refinement for $[Cu(L)(NO_3)]NO_3 \cdot H_2O$.

Empirical formula	$C_{22}H_{24}CuN_8O_9S_2$
Formula weight	672.15
Temperature	298(2) K
Wavelength	0.71073 Å
Crystal system	Monoclinic
Space group	*C2/c*
Unit cell dimensions	a = 18.4094(8) Å, α = 90°
	b = 15.6079(8) Å, β = 112.336(4)°
	c = 23.7095(13) Å, γ = 90°
Volume	6301.4(5) $Å^3$
Z	8
Density (calculated)	1.417 mg/m^3
Absorption coefficient	0.884 mm^{-1}
F(000)	2760
Crystal size	0.12 × 0.08 × 0.06 mm^3
Theta range for data collection	2.89–25.00°
Index ranges	$-21 \le h \le 21, -18 \le k \le 18, -28 \le l \le 28$
Reflections collected	40,794
Independent reflections	5543 [R(int) = 0.0720]
Completeness to θ = 25.00°	99.8%
Absorption correction	Semi-empirical from equivalents
Max. and min. transmission	0.9489 and 0.9014
Refinement method	Full-matrix least-squares on F^2
Data/restraints/parameters	5543/2/378
Goodness-of-fit on F^2	1.075
Final R indices [$I>2\sigma(I)$]	R_1 = 0.0779, wR_2 = 0.2236
R indices (all data)	R_1 = 0.1055, wR_2 = 0.2431
Largest diff. peak and hole	0.951 and −0.509 e $Å^{-3}$

Table 2. Selected bond lengths (Å) and angles (°) for $[Cu(L)(NO_3)]NO_3$.

Cu(1)–N(6)	1.950(5)	N(6)–Cu(1)–N(2)	173.9(2)
Cu(1)–N(2)	1.974(5)	N(6)–Cu(1)–O(1)	94.06(19)
Cu(1)–O(1)	2.061(4)	N(2)–Cu(1)–O(1)	85.91(19)
Cu(1)–O(2)	2.157(5)	N(6)–Cu(1)–O(2)	90.35(19)
Cu(1)–O(3)	2.176(8)	N(2)–Cu(1)–O(2)	95.73(19)
Cu(1)–O(4)	2.433(7)	O(1)–Cu(1)–O(2)	96.60(19)
S(1)–S(2)	2.025(3)	O(1)–Cu(1)–O(3)	165.8(2)
		O(2)–Cu(1)–O(3)	97.0(2)
		O(1)–Cu(1)–O(4)	113.2(2)

3. Results and discussion

3.1. *Crystal structure description*

The ORTEP diagram of $[Cu(L)NO_3]NO_3 \cdot H_2O$ with atomic numbering scheme is shown in figure 1. The complex crystallizes in the monoclinic *C2/c* space group with one molecule in the asymmetric unit. The copper in $[Cu(L)NO_3]NO_3 \cdot H_2O$ adopts a distorted octahedral geometry. The ligand provides four coordination sites through two benzimidazole imine nitrogens, N2 and N6 (Cu(1)–N(6) = 1.950(5) and Cu(1)–N(2) = 1.974(5) Å), and two amide carbonyl oxygens, O1 and O2 (Cu(1)–O(1) = 2.061(4) and Cu(1)–O(2) = 2.157(5) Å). The remaining two coordination sites O3 and O4 are provided by bidentate nitrate (Cu(1)–O(3) = 2.176(8) Å and Cu(1)–O(4) = 2.433(7) Å). The third uncoordinated oxygen atom of the bound nitrate was disordered over two positions O5B and O5A (disordered ratio 67:33, respectively). A comparative study of bond lengths and angles is given in table 2. One nitrate is present in the crystal lattice to balance the charge. A highly disordered water is also present in the lattice for which the disorder could not be modeled and it was refined only isotropically.

3.2. *PXRD studies*

As suitable single crystals for [Cu(L)Cl]Cl could not be grown, the powder XRD pattern of the compound was matched with $[Cu(L)NO_3]NO_3$ with lattice constant a = 18.4094, b = 15.6079, c = 23.7095, α = 90.00, β = 112.336, γ = 90.00; monoclinic, *C2/c*.

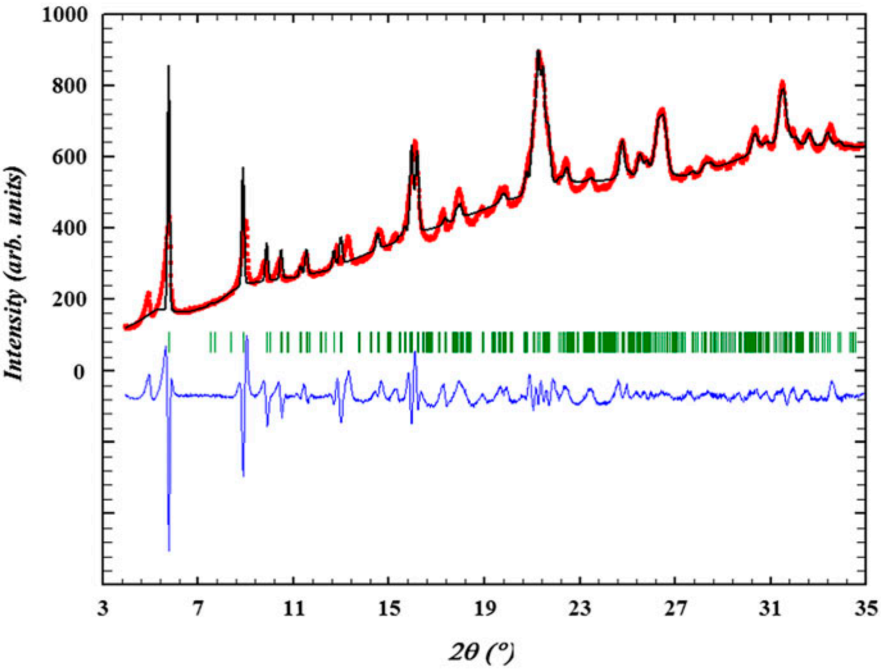

Figure 2(a). PXRD pattern of [Cu(**L**)Cl] and Le-Bail fit of the powder X-ray diffraction pattern. Red (observed), black (Calc), blue (Obs Calc), vertical line (Bragg reflection) (see http://dx.doi.org/10.1080/00958972.2013.835403 for color version).

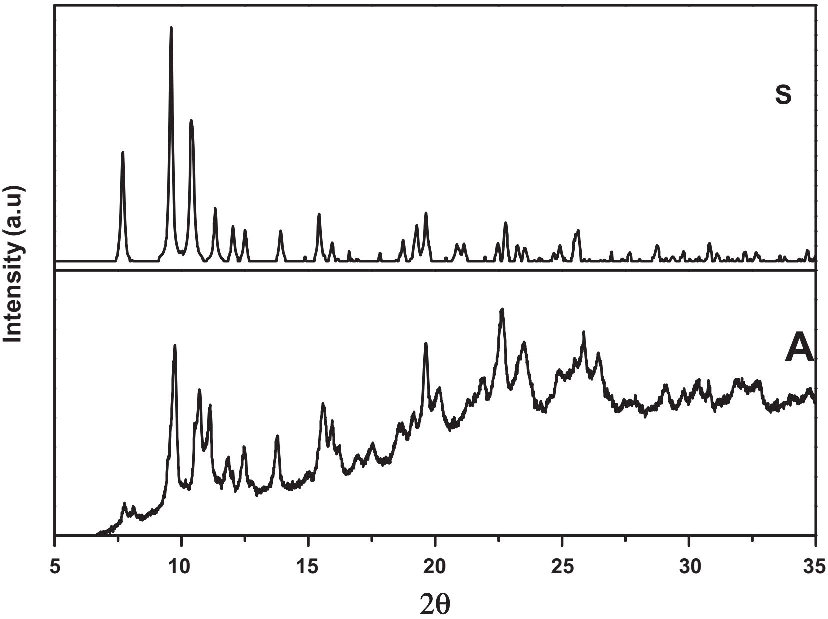

Figure 2(b). (A) Powder XRD pattern of Cu(L)NO_3. (S) Simulated pattern obtained from single crystal data.

The Le-Bail fit of the powder X-ray diffraction pattern of [Cu(L)Cl]Cl (figures 2(a) and (b)) yielded the lattice constant a = 18.2124, b = 15.6691, c = 33.0812, α = 90.00, β = 112.1068, γ = 90.00; monoclinic, *C2/c*.

On the basis of a close fit of the a, b, c and α, β, γ parameters with that for [Cu(L)NO_3]NO_3, it is proposed that [Cu(L)Cl]Cl also has a similar lattice structure [14].

3.3. *Characterizations*

3.3.1. ^{1}H NMR spectra. The ^{1}H NMR spectra of the ligands were measured in d_6-DMSO. The benzimidazolyl N–H protons appear as a singlet at 12.2 ppm. The protons due to amide N–H give a triplet at 8.70–8.67 ppm. The benzene protons which are adjacent to benzimidazole N–H appear as a quartet at 7.14–7.13 ppm and the remaining benzene protons show a doublet at 7.53–7.45 ppm. The protons of $-CH_2-$ attached to the amide appear as a doublet at 4.50–4.47 and protons of $-CH_2-CH_2-$ appear as triplets at 2.97–2.93 and 2.63–2.61 ppm, respectively (Supplementary material).

3.3.2. Mass spectra analysis. A main peak was found in the ESI/MS$^+$ at 468 that corresponds to the molecular ion peak for L.

3.3.3. Electronic spectroscopy. The electronic spectra of all the Cu(II) complexes show two peaks at 276–287 nm. These peaks are assigned to the π–π* transition of benzimidazole in the ligands [15]. Absorption at this position is high as indicated by their extinction coefficient. The Cu(II) complexes exhibit a single symmetrical but broad *d–d* band in the region 700–770 nm, characteristic of copper(II) in a tetragonal geometry [16]. These bands are assigned to the transition d_{xz}, $d_{yz} \rightarrow d_{x2-y2}$, and $d_{xy} \rightarrow d_{x2-y2}$. The difference in absorption band position may be due to the ligand field splitting of the coordinated ligand. The decrease in the energy of the absorption maxima on going from $[Cu(L)NO_3]NO_3$ to $[Cu(L)Cl]Cl$ in these complexes can be attributed to a decrease in the plane ligand field splitting which reflects different degrees of distortions of copper(II) bound to the ligands.

3.3.4. IR spectral studies. IR stretching bands for the ligand and complexes are listed in table 3. A broad band at 3300–3500 cm^{-1} in ligand and complexes indicates the presence of associated H_2O molecules. Small shifts are observed for the C–S stretch, while shifts in amide I and amide II stretches due to the –CO–NH– group indicate the coordination of the ligand through the carbonyl oxygen present in the ligands [14, 17]. The nitrate complex shows bands between 1372 and 830 cm^{-1} due to $\nu_{O–N–O}$ symmetric and $\nu_{O–N–O}$ anti-symmetric stretching of the coordinated nitrate [18].

3.3.5. Molar conductance. The molar conductivity values were measured in DMF. The values are $37.2\,\Omega^{-1}\,cm^2\,M^{-1}$ and $48.0\,\Omega^{-1}\,cm^2\,M^{-1}$ for $[Cu(L)Cl]Cl$ and $[Cu(L)NO_3]NO_3$, respectively. This indicates that at least one anion (chloride/nitrate) is dissociated in solution [19].

3.3.6. Cyclic voltammetry. Cyclic voltammograms of the copper(II) complexes were recorded in DMSO. The Cu(II) complexes show a quasi reversible redox wave (Supplementary material) due to the Cu(II)/Cu(I) couple (table 4). Anodic shifts in $E_{1/2}$ values indicate retention of the anion in the coordination sphere of Cu(II). $E_{1/2}$ values become cathodic in the order $Cl^- < NO_3^-$ for the ligand L. Earlier reported $E_{1/2}$ values of the benzimidazole-based Cu(II) complexes [16, 20, 21] are less positive than for the present complexes. Copper(II) complexes of *bis*-benzimidazolyl thioether with five-membered chelate rings show that the potential increases with increase in the number of thioether donors [22, 23].

Table 3. IR spectral data of ligands and Cu(II) complexes.

Assignments (cm^{-1}) complexes	ν_{OH} stretch	ν_{NH} amide	ν_{NH} benzimi	$\nu_{C=O}$ amide I	$\nu_{C=O}$ amide II	$\nu_{–C=C–N=C}$ group freq	ν special for anions	$\nu_{benz.}$	$\nu_{C–S}$ stretch
Ligand [L]	3310	3235	3062	1646	1540	1426	–	740	677
$[Cu(L)Cl_2]$	3421	3250	3065	1654	1540	1455	–	745	663
$[Cu(L)(NO_3)_2]$	3450	3257	3058	1625	1543	1453	1384	745	663

Table 4. Electrochemical data of the Cu(II) complexes.

Complexes	E_c (mV)	E_a (mV)	$E_{1/2}$ (mV)*
$[Cu(L)Cl_2]$	−138	−41	−48.5
$[Cu(L)(NO_3)_2]$	−254	+116	−69

*Values with respect to Fc/Fc^+ of + 56 mV.

The present $E_{1/2}$ values are also more cathodic than those previously reported for benzimidazolyl amide-based complexes [12, 23b]. Thus it may be concluded that there could be a role of the sulfur in the ligating system for stabilizing the Cu(II) complexes.

3.3.7. EPR Data. X-band EPR spectra of the copper(II) complexes were recorded in DMF (Supplementary material and table 5). Solution spectra of both copper complexes typically indicate a d_{x2-y2} ground state ($g_{||} > g_{\perp} > 2.0023$). EPR spectra of some Cu(II) complexes show less than four lines and broadening of $g_{\perp}$ line, indicating a severe distortion of tetragonal geometry [24]. The values of hyperfine coupling constant $A_{||}$ are also low in comparison to the normal range found for other copper(II) complexes. Further, no nitrogen super hyperfine splitting could be observed, implying non-planarity of the complexes. The values of $g_{||}/A_{||}$ follow the order $[Cu(L)NO_3]NO_3$~$[Cu(L)Cl]Cl$, implying a similar solution structure for both the complexes.

3.3.8. Fluorescence. Figure 3 shows the solvent dependence of fluorescence (λ_{exc} 277 nm) for L in MeOH, DMF, and MeCN. The intensity of the emission at ~297 nm is attributed to benzimidazolyl in the ligand that is a known fluorophore [25]. λ_{max} of the emission band slightly shifts in various solvent systems in the range ~295–297 nm (figure 3(a)). These small shifts are indicative of varying degrees of solvation of the excited state and imply that there is minimal change in the dipole moment of the fluorophore in the excited state, with

Table 5. X-band EPR data of the Cu(II) complexes.

Complexes	$A_{\|\|}$	$g_{\|\|}$	$g_{\perp}$	α^2	$g_{\|\|}/A_{\|\|} \times 10^4$
$[Cu(L)Cl_2]$	143	2.28	2.07	0.558	160
$[Cu(L)\ (NO_3)_2]$	147	2.33	2.07	0.702	159

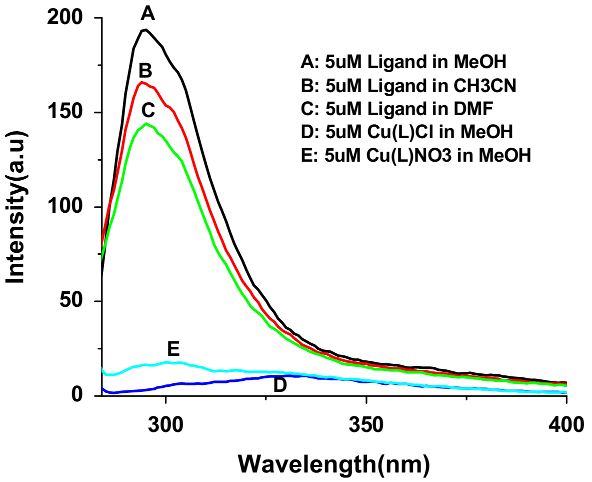

Figure 3(a). Fluorescence spectrum of L (curves A–C) in different solvents. Curves D and E represent the fluorescence of respective complexes in methanol.

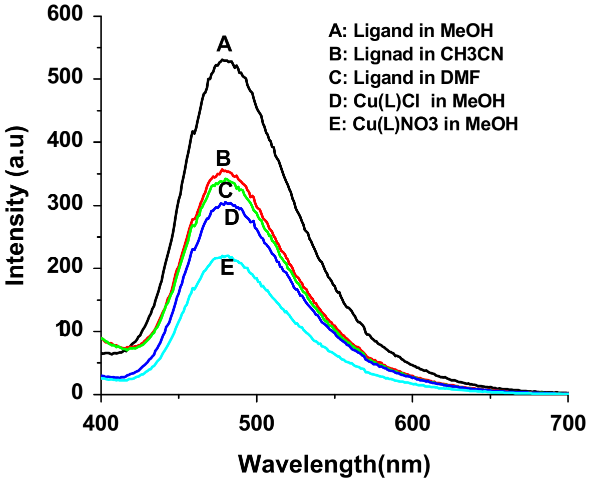

Figure 3(b). Fluorescence spectrum (480 nm) of L (curves A–C) in different solvents. Curves D and E represent the fluorescence of respective complexes in methanol.

varying solvent system [26]. The emission intensity for *L* decreases in the order MeOH > MeCN > DMF, showing a loss of almost 27% from MeOH to DMF (figure 3(a)). The fluorescence quenching is strongly affected by the nature of the solvent. Quenching is higher in DMF than in MeOH and CH_3CN. As PET-mediated quenching occurs relatively more rapidly in a polar solvent, the quenching effect can be attributed to a PET process [27]. Fluorescence spectra also reveal the presence of an emission band at ~487 nm (figure 3(b)); small shifts are observed with change in the solvent system. Quenching of this band is again largest in the more polar DMF in comparison to MeOH.

The fluorescence emission spectra of the respective complexes [Cu(L)Cl]Cl and $[Cu(L)NO_3]NO_3$ were recorded in MeOH, showing a nearly complete quenching of the emission band at ~297 nm observed in the free ligand (figure 3(a)), and a quenching of nearly 40–60% is found in the emission band at 487 nm (figure 3(b)). Such a quenching is attributed to the CHEQ effect; however since the geometry of the two complexes is the same, the role of the anion in the quenching process (chloride *vs.* nitrate) cannot be ruled out.

4. Catalytic studies of $[Cu(L)NO_3]NO_3$

4.1. *Oxidation of alcohol*

A number of catalytic systems have been reported that oxidize aryl and alkyl-based alcohols to the corresponding carbonyl compounds. These include Ru(II) carbonyl [28] and phenanthroline complexes [29] that mainly use N-methyl morpholine oxide and $NaIO_4$ as respective oxidants with product yields from 74 to 98%. Cu(II) azo [30] and a Ni Schiff base complex [31] have also been utilized for the oxidation of benzyl, piperonyl, cinnamyl, and a variety of alkyl and benzyl alcohols. Oxidants used were H_2O_2 and periodic acid, respectively, and product yields vary between 60 and 90%. Cr(VI) has been utilized for the oxidation of sugars, ethane, and propane diols in miceller media [32]. Selective oxidation of benzylic alcohol has been reported using a hybrid catalyst, substituted polyoxometalates using oxidants H_2O_2, periodic acid and *tert*-butyl-hydroperoxide. Yields of about 100% were reported with H_2O_2 while they were only 48% for *tert*-butyl-hydroperoxide [33].

We have utilized the present copper(II) complex $[Cu(L)NO_3]NO_3$ to catalyze the oxidation of pyridyl and naphthyl alcohols using TBHP as an alternative source of active oxygen for which few reports are available [29, 34].

4.2. *General procedure*

The complex (10 mg) was dissolved in MeOH (5 mL) and methanolic solution (5 mL) of substrates (various alcohols) and 0.02 mL of TBHP was added. The ratio of catalyst: substrate:TBHP was 1:20:20. The reaction mixture was stirred at 45 °C on a water bath for 12 h. The reaction mixture was analyzed by TLC. The reaction mixture was evaporated to near dryness on a rotary evaporator and extracted with dichloromethane. The products in this extracted reaction mixture were analyzed using GCMS.

When the same reaction was performed without complex, no product could be obtained during the same period, implying that $[Cu(L)NO_3]NO_3$ catalyzes the oxidation of alcohols to the corresponding aldehydes. The general reaction may be represented as follows:

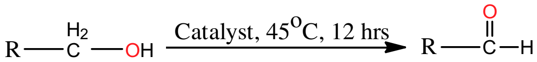

$$R-\overset{H_2}{C}-OH \xrightarrow{\text{Catalyst, }45^{o}\text{C, 12 hrs}} R-\overset{O}{\overset{\|}{C}}-H$$

4.3. *Oxidation of alcohols using $[Cu(L)NO_3]NO_3$*

4.3.1. Oxidation of 3-pyridyl carbinol. 3-Pyridyl carbinol oxidizes to form nicotinaldehyde (82.0%, mol. weight 107) and nicotinic acid (18.0%, mol. weight 123). These two products were found at retention times 10.4 and 14.8 using GCMS technique (table 6).

4.3.2. Oxidation of 1,2,3,4-tetrahydronaphthol. 1,2,3,4-Tetrahydronaphthol (mol. weight 148, retention time 16.0) oxidizes to form 3,4-tetrahydronaphthalenal-(2H)-one (56.9%). This product was found at retention times 16.4 and 28.1 (two isomeric forms, mol. weight 146) using the GCMS technique (table 6).

4.3.3. Oxidation of 4-methoxybenzyl alcohol. 4-Methoxybenzyl alcohol (mol. weight 138, retention time 14.3) oxidizes to form 4-methoxybenzaldehyde (mol. weight 136) (15.4%) and 4-methoxybenzoic acid (mol. weight 152) (8.22%). These two products were found at retention times 13.8 and 15.4 using the GCMS technique (table 6).

4.3.4. Oxidation of 4-nitrobenzyl alcohol. 4-Nitrobenzyl alcohol (mol. weight 153, retention time 21.9) oxidizes to form 4-nitrobenzaldehyde (mol. weight 151) (4.9%) and 4–nitrobenzoic acid (mol. weight 166) (11.0%). These two products were found at retention times 18.0 and 21.5 using the GCMS technique (table 6).

Table 6. Oxidation products of alcohols using [Cu(L)(NO$_3$)]·NO$_3$.

Substrates		Products		Retention time (min)	Yield
3-Pyridyl carbinol	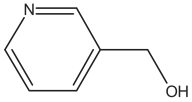	Nicotinaldehyde	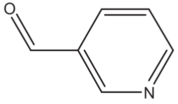	10.4	82.0 (%)
		Nicotinic acid	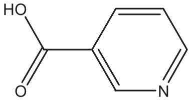	14.8	18.0 (%)
1,2,3,4-Tetrahydronaphthol	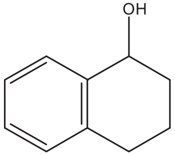	3,4-Dihydronaphthalen-1(2H)-one	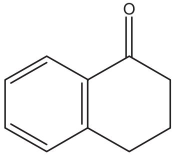	16.4	56.9 (%)
4-Methoxybenzyl alcohol	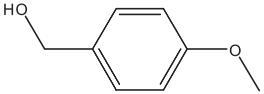	4-Methoxybenzaldehyde	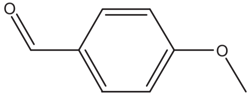	13.8	15.4 (%)
		4-Methoxybenzoic acid	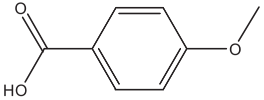	15.4	8.2 (%)
4-Nitrobenzyl alcohol	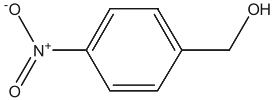	4-Nitrobenzaldehyde	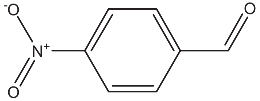	18.0	4.9 (%)
		4-Nitrobenzoic acid	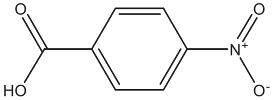	21.5	11.0 (%)

5. Conclusion

The present work describes the synthesis and characterization of a new $N_2O_2S_2$ donor benzimidazolyl-based ligand (L) and its copper(II) complexes. The main peak in the ESI/MS$^+$ at 468 corresponds to the molecular ion peak for L. SCXRD on $[Cu(L)NO_3]NO_3 \cdot H_2O$ reveals that copper has a distorted octahedral geometry. The ligand provides four coordination sites while the remaining two coordination sites are provided by a bidentate nitrate. One nitrate group is uncoordinated, supported by molar conductance data which indicate that at least one anion is dissociated in solution. The presence of nitrate is supported by bands in the IR spectra. The a, b, c and α, β, γ parameters obtained from the powder XRD of [Cu(L)Cl]Cl were matched with that of $[Cu(L)NO_3]NO_3$ and a close fit suggests that both possess a similar lattice structure.

The Cu(II) complexes exhibit a broad *d–d* band at 700–790 nm, characteristic of copper(II) in a tetragonal geometry. Cyclic voltammograms show that the $E_{1/2}$ values are more cathodic than previously reported for benzimidazolyl amide-based complexes. Anodic shifts in $E_{1/2}$ indicate the retention of an anion in the coordination sphere of Cu(II). EPR spectra of both copper complexes indicate a d_{x2-y2} ground state ($g_{||} > g_{\perp} > 2.0023$). The values of the hyperfine coupling constant $A_{||}$ are low, implying non-planarity of the complexes. The fluorescence emission intensity for L decreases in the order MeOH > MeCN > DMF, while the emission spectra of the respective complexes show a nearly complete quenching of the emission band at ~297 nm in the free ligand. Such quenching is attributed to the CHEQ effect. $[Cu(L)NO_3]NO_3$ is used to catalyze the oxidation of pyridyl, naphthyl, and benzyl alcohols, with highest yields and high selectivity for pyridyl carbonyl oxidation, in comparison to naphthyl and benzyl alcohols.

Supplementary material

Crystal data in CIF format for $[Cu(L)(NO_3)]NO_3 \cdot H_2O$. CCDC-921436 contain the Supplementary crystallographic data for this article. These data can be obtained free of charge from the Cambridge Crystallographic Data Center via www.ccdc.cam.ac.uk/data_request/cif.

Acknowledgment

We gratefully acknowledge the financial support from the University of Delhi for a special grant. Thanks to AIRF (JNU) for the GCMS data.

References

[1] M. Hakimi, H. Vahedi, R. Takjoo, A. Rezaeifard. *Int. J. Chem. Tech. Res.*, **4**, 1658 (2012).
[2] P.U. Maheswari, F. Hartl, M. Quesada, F. Buda, M. Lutz, A.L. Spek, P. Gamez, J. Reedijk. *Inorg. Chim. Acta*, **374**, 406 (2011).
[3] Y.D. Wang, T.D.P. Stack. *J. Am. Chem. Soc.*, **118**, 13097 (1996).
[4] P. Chaudhuri, M. Hess, J. Muller, K. Hildenbrand, E. Bill, T. Weyhermuller, K. Wieghardt. *J. Am. Chem. Soc.*, **121**, 9599 (1999).
[5] J.S. Panek, C.E. Masse. *Angew. Chem., Int. Ed.*, **38**, 1093 (1999).

[6] V.B. Valodkar, G.L. Tembe, M. Ravindranathan, R.N. Rama, H.S. Rama. *J. Mol. Catal. A: Chem.*, **208**, 21 (2004).

[7] A. Corma, H. Garcia. *Chem. Rev.*, **102**, 3837 (2002).

[8] L.F. Loita, A.M. Venezia, G. Deganello, A. Longo, A. Martorana, Z. Schay, L. Guczi. *Catal. Today*, **66**, 271 (2001).

[9] V.R. Choudhary, A. Dhar, P. Jana, R. Jha, B.S. Uphade. *Green Chem.*, **7**, 768 (2005).

[10] (a) S. Striegle. *Tetrahedron*, **62**, 9109 (2006); (b) G. Ferguson, A.N. Ajjou. *Tetrahedron Lett.*, **44**, 9139 (2003).

[11] L.A. Cescon, A.R. Day. *J. Org. Chem.*, **27**, 581 (1962).

[12] M. Gupta, P. Mathur, R.J. Butcher. *Inorg. Chem.*, **40**, 878 (2001).

[13] (a) G.M. Sheldrick. *SHELXS-97 and SHELXL-97, Program for Crystal Structure Solution and Refinement*, University of Gottingen, Germany (1997); (b) L.J. Farrugia, WinGX suite for small-molecule single-crystal crystallography. *J. Appl. Crystallogr.*, **32**, 837 (1999).

[14] J.K. Clegg, L.F. Lindoy, J.C. McMurtrie, D. Schilter. *Dalton Trans.*, 3114 (2006).

[15] R. Bakshi, M. Rossi, F. Caruso, P. Mathur. *Inorg. Chim. Acta*, **376**, 175 (2011).

[16] E. Monanzani, L. Quinti, A. Perotti, L. Casella, M. Gulloti, L. Randaccio, S. Geremia, G. Nardin, P. Faleschini, G. Tabbi. *Inorg. Chem.*, **37**, 553 (1998).

[17] G. Ahuja, P. Mathur. *Inorg. Chem. Commun.*, **17**, 42 (2012).

[18] S. Menage, L. Que Jr. *Inorg. Chem.*, **29**, 4293 (1990).

[19] S. Pal, S.N. Poddar, S. Ghosh, G. Mukherjee. *Polyhedron*, **14**, 3023 (1995).

[20] T. Sakurai, H. Oi, A. Nakahara. *Inorg. Chim. Acta*, **92**, 131 (1984).

[21] M. Palaniandavar, T. Pandiyan, M. Laxminarayan, H. Manohar. *J. Chem. Soc., Dalton Trans.*, 457 (1995).

[22] U. Sivagnanam, M. Palaniandavar. *J. Chem. Soc., Dalton Trans.*, 2277 (1994).

[23] (a) N. Tyagi, P. Mathur. *Spectrochim. Acta, Part A*, **96**, 759 (2012); (b) S. Tehlan, M.S. Hundal, P. Mathur. *Inorg. Chem.*, **43**, 6589 (2004).

[24] G. Batra, P. Mathur. *Inorg. Chem.*, **31**, 1575 (1992).

[25] (a) R. Khatter, P. Mathur. *Inorg. Chim. Acta.*, **31**, 37 (2013); (b) K. Mahiya, P. Mathur. *Spectrochim. Acta*, **113**, 386 (2013).

[26] N. Ghoneim. *Spectrochim. Acta, Part A*, **57**, 1873 (2001).

[27] M. Formica, V. Fusi, L. Giorgi, M. Micheloni. *Coord. Chem. Rev.*, **256**, 170 (2012).

[28] N. Gunasekaran, N. Remya, S. Radhakrishnan, R. Karvembu. *J. Coord. Chem.*, **64**, 491 (2011).

[29] S.J. Bozorghi, H. Esfandiari, H. Saravani, F.R. Charati, B.W. Skelton, M. Makha. *J. Coord. Chem.*, **65**, 994 (2012).

[30] A.G.F. Shoair. *J. Coord. Chem.*, **65**, 3551 (2012).

[31] R. Rajarao, T.H. Kim, B.R. Bhat. *J. Coord. Chem.*, **65**, 2671 (2012).

[32] S.K. Ghosh, A. Basu, R. Saha, A. Ghosh, K. Mukherjee, B. Saha. *J. Coord. Chem.*, **65**, 1158 (2012).

[33] Z. Nadealian, V. Mirkhani, B. Yadollahi, M. Moghadam, S. Tangestaninejed, I. Mohammadpoor-Baltork. *J. Coord. Chem.*, **65**, 1071 (2012).

[34] S.C. Mahapatra, S. Tehlan, M.S. Hundal, P. Mathur. *Inorg. Chim. Acta*, **361**, 1897 (2008).